

# Journal of Materials Chemistry B

Accepted Manuscript



This is an *Accepted Manuscript*, which has been through the Royal Society of Chemistry peer review process and has been accepted for publication.

*Accepted Manuscripts* are published online shortly after acceptance, before technical editing, formatting and proof reading. Using this free service, authors can make their results available to the community, in citable form, before we publish the edited article. We will replace this *Accepted Manuscript* with the edited and formatted *Advance Article* as soon as it is available.

You can find more information about *Accepted Manuscripts* in the [Information for Authors](#).

Please note that technical editing may introduce minor changes to the text and/or graphics, which may alter content. The journal's standard [Terms & Conditions](#) and the [Ethical guidelines](#) still apply. In no event shall the Royal Society of Chemistry be held responsible for any errors or omissions in this *Accepted Manuscript* or any consequences arising from the use of any information it contains.

**Stable polymersomes based on ionic-zwitterionic block copolymers modified with superparamagnetic iron oxide nanoparticles for biomedical applications†**

Gabriela Kania,<sup>a</sup> Urszula Kwolek,<sup>a</sup> Keita Nakai,<sup>b</sup> Shin-ichi Yusa,<sup>b</sup> Jan Bednar,<sup>cd</sup> Tomasz Wójcik,<sup>e</sup> Stefan Chłopicki,<sup>ef</sup> Tomasz Skórka,<sup>g</sup> Michał Szuwarzyński,<sup>a</sup> Krzysztof Szczubiałka,<sup>a</sup> Mariusz Kepczynski,<sup>\*a</sup> Maria Nowakowska<sup>\*a</sup>

<sup>a</sup> Faculty of Chemistry, Jagiellonian University in Kraków, Ingardena 3, Kraków 30-060, Poland, fax no.: +4812 6340515, e-mail: [kepczyns@chemia.uj.edu.pl](mailto:kepczyns@chemia.uj.edu.pl), [nowakows@chemia.uj.edu.pl](mailto:nowakows@chemia.uj.edu.pl)

<sup>b</sup> Department of Materials Science and Chemistry, Graduate School of Engineering, University of Hyogo, 2167 Shosha, Himeji, Hyogo 671-2280, Japan

<sup>c</sup> University of Grenoble 1/CNRS, LIPhy UMR 5588, 140 Av. de la Physique, Grenoble, F-38041, France

<sup>d</sup> Charles University in Prague, First Faculty of Medicine, Institute of Cellular Biology and Pathology, Albertov 4, 128 01 Prague 2, Czech Republic

<sup>e</sup> Jagiellonian Centre for Experimental Therapeutics (JCET), Jagiellonian University in Kraków, Bobrzyńskiego 14, Kraków 30-348, Poland

<sup>f</sup> Chair of Pharmacology, Jagiellonian University Medical College, Grzegórzecka 16, Kraków 31-531, Poland

<sup>g</sup> Department of Magnetic Resonance Imaging, Institute of Nuclear Physics, Polish Academy of Sciences, Radzikowskiego 152, Kraków 31-342, Poland

† Electronic supplementary information (ESI) available.

## Abstract

Stable polymersomes with semipermeable membranes were prepared by simple mixing two oppositely charged diblock copolymers containing zwitterionic and cationic (PMPC<sub>20</sub>-*b*-PMAPTAC<sub>190</sub>) or anionic (PMPC<sub>20</sub>-*b*-PAMPS<sub>196</sub>) blocks. The formation of vesicular structures in the mixed solution of the block copolymers was confirmed by direct observation with cryo-TEM technique. Superparamagnetic iron oxide nanoparticles coated with cationic chitosan derivative (SPION/CCh) and these decorated with a fluorescent probe molecule were next incorporated into the polymersome structure. The average diameter of SPION/CCh-polymersomes estimated with cryo-TEM was about 250 nm. Surface topography of the SPION/CCh-loaded vesicles was imaged using AFM and magnetic properties of these objects were confirmed by MFM and MRI measurements. The ability of the SPION/CCh-polymersomes to affect T<sub>2</sub> relaxation time in MRI was evaluated based on the measurements of  $r_2$  relaxivity. The obtained value of  $r_2$  ( $573 \pm 10 \text{ mM}^{-1}\text{s}^{-1}$ ) was quite high. The cytotoxicity and intracellular uptake of the SPION/CCh-loaded vesicles into EA.hy926 cells were studied. The results indicate that the SPION/CCh-polymersomes seem to be internalized by vascular endothelium and are not cytotoxic to endothelial cells up to 1  $\mu\text{g Fe/ml}$ . Therefore, it can be suggested that the SPION/CCh-polymersomes could prove useful as T<sub>2</sub> contrast agents in MRI of endothelium.

Keywords: polymersome; endothelial cell; MRI; copolymer; biocompatibility; self assembly; superparamagnetic iron oxide nanoparticles

## 1. Introduction

There has been a growing interest in the application of polymeric vehicles, called polymersomes,<sup>1</sup> as nanocarriers in biomedicine. Polymersomes are structures analogous to liposomes, formed in the self-assembly process from synthetic amphiphilic block copolymers containing hydrophilic and hydrophobic blocks. They show higher colloidal stability, better mechanical properties, higher drug loading capacity, longer blood circulation time, lower drug leakage and greater storage capability than liposomes.<sup>2-5</sup> To improve the control over the cargo release, the stimuli-sensitive components were incorporated into the polymersome structure. Such polymeric vehicles respond to internal or external stimuli, including: pH, redox potential, temperature, ultraviolet or near-infrared light, carbon dioxide, enzymes, magnetic field, and ultrasound, either reversibly or irreversibly.<sup>6-8</sup> However, the hydrophobic membrane of polymersomes prepared from the amphiphilic polymers restricts the penetration of the hydrophilic solutes, thereby limiting their function as semipermeable container systems. To solve that problem the researchers have used the aforementioned pH-sensitive polymersomes<sup>9,10</sup> or have prepared the semipermeable membrane by simple mixing of a pair of oppositely charged block copolymers (PICsomes) in an aqueous medium.<sup>11</sup> Additionally, the latter approach facilitates the encapsulation of unstable compounds such as proteins without using any organic solvents.

Although the idea of applying magnetic field in medicine is quite old,<sup>12</sup> the practical protocols are still not fully developed. There is considerable interest in the improvement in the sensitivity and safety of the contrast agents. So far, two main types of magnetic resonance contrast agents, *i.e.*, gadolinium compounds<sup>13</sup> and superparamagnetic iron oxide nanoparticles (SPION),<sup>14</sup> have been prepared as colloidal aqueous dispersion or incorporated into polymeric membranes. It was shown that SPION could be incorporated into polymersomes formed by self-assembly of various amphiphilic block copolymers.<sup>14,15,16,17,18</sup> Possible

biomedical applications of such magnetically sensitive polymersomes include magnetic resonance imaging (MRI), hyperthermia, magnetically guided transport to diseased tissues<sup>19</sup> and controlled drug release in the target tissue triggered by an external alternating magnetic field.<sup>20</sup> Moreover, the possibility of further functionalization, *e.g.*, by the covalent attachment of targeting peptides and/or fluorescent labels can be considered to broaden possible applications.<sup>21-23</sup>

The vascular endothelium is regarded today as a major endocrine/paracrine/autocrine organ that plays a fundamental role in the regulation of the cardiovascular system. Indeed, endothelium via plethora of mediators, including nitric oxide (NO), prostacyclin (PGI<sub>2</sub>) carbon monoxide (CO) and adenosine regulates vascular tone, vascular wall permeability, vascular structure as well as is involved in inflammation and thrombosis.<sup>24</sup> There is overwhelming evidence that endothelial dysfunction promotes the development of atherothrombosis, diabetes, and many other diseases and its diagnosis possesses prognostic significance.<sup>25</sup> Accordingly, pharmacotherapy of endothelium, and localized drugs delivery to endothelium in particular, offer a novel therapeutic approach to various cardiovascular diseases.<sup>26</sup> Few systems have been previously used to target therapeutic agents to endothelium. A drug-conjugate, such as  $\beta$ -Gal enzyme attached to anti-PECAM (PECAM is a highly expressed endothelial surface antigen), was accumulated in the lungs and induced a marked elevation of  $\beta$ -Gal activity in the lung tissue, and thus may be potentially useful for the treatment of acute pulmonary or vascular diseases.<sup>27</sup> Immunoliposomes, *e.g.* sialyl Lewis<sup>x</sup>-liposomes, were used to deliver antisense oligonucleotides (AS-ODNs) directed against the adhesion molecule ICAM-1 to activated vascular endothelial cells.<sup>28</sup>

In this study, we report for the first time on the application of PICsomes, the stable polymersomes with the semipermeable membrane, as a useful carrier of SPION, an MRI contrast agent. For that purpose, two novel oppositely charged well-defined and

biocompatible diblock copolymers were designed and synthesized in a two-step procedure. The copolymers comprised the zwitterionic block with phosphorylcholine groups and the cationic or anionic block. The formation of vesicular structures in the appropriate mixture of aqueous solutions of the copolymers was confirmed by the direct visualization with cryo-transmission electron microscopy. Next, SPION coated with a cationic chitosan derivative (SPION/CCh) were incorporated into the membrane and/or interior of the polymersomes. Magnetic properties of SPION/CCh-polymersomes were evaluated using AFM/MFM techniques and contrast enhancement ability in MRI was confirmed by the relaxation time measurements. *In vitro* cytotoxicity and intracellular uptake by endothelium were studied on EA.hy926 cells using MTT assay and CLSM, respectively. The results suggest that polymersomes composed of the pair of oppositely charged block copolymers, when used as carriers for incorporated SPION/CCh contrast agents, may prove useful as MRI contrast agents. Importantly, since SPION/CCh-polymersomes were up-taken by the endothelium, we suggest their potential use as a delivery system to endothelium.

## 2. Experimental section

### 2.1. Chemicals and cell culture

All chemicals were obtained from commercial sources (Sigma-Aldrich, Life Technologies) and used without further purification. Chitosan (low molecular weight, Sigma-Aldrich) was cationically modified (CCh) by reaction with glycidyltrimethylammonium chloride (GTMAC) as previously described,<sup>29</sup> the degree of substitution of chitosan with quaternary ammonium groups was ca. 57%. 4-Cyanopentanoic acid dithiobenzoate (CPD) was synthesized as previously described.<sup>30</sup> 4,4'-Azobis(4-cyanopentanoic acid) (V-501, 98%) was obtained from Wako Chemicals. SHP-20, the commercial MRI contrast agent, was

obtained from Ocean NanoTech. Millipore-quality water was used for all solution preparations.

A hybridoma EA.hy926 cell line, formed by the fusion of HUVEC with an A549 human lung carcinoma cell line, was kindly provided by Dr. C-J. Edgell (Department of Pathology, University of North Carolina, Chapel Hill, NC, USA).<sup>31</sup> The cells were grown in Dulbecco's Modified Eagle Medium (DMEM) containing 4.5 mg per ml glucose, 10% fetal bovine serum, 100 U per ml penicillin, 100  $\mu$ g per ml streptomycin and 2% HAT supplement (complete culture medium), maintained at 37°C in a fully humidified atmosphere of 5% CO<sub>2</sub> and passaged twice a week.

## **2.2. Syntheses of diblock copolymers, PMPC<sub>20-b</sub>-PMAPTAC<sub>190</sub> and PMPC<sub>20-b</sub>-PAMPS<sub>196</sub>**

Poly(2-(methacryloyloxy)ethyl phosphorylcholine) (PMPC) macro-chain transfer agent (PMPC macro-CTA) was synthesized according to the modified previously reported method.<sup>32</sup> MPC (6.03 g, 20.4 mmol) was dissolved in 38.8 mL of mixed methanol and water (7/5, v/v), and then CPD (423 mg, 1.38 mmol) and V-501 (48.0 mg, 0.171 mmol) were added to the solution. The aqueous solution was degassed by purging with Ar gas for 30 min. Polymerization was carried out at 70°C for 6 h. The reaction mixture was dialyzed against pure water for 2 days. PMPC was recovered by freeze-drying (6.05 g, 93.8%). The number-average molecular weight ( $M_n$ ) and dispersity index ( $M_w/M_n$ ) estimated from gel-permeation chromatography (GPC) were  $6.21 \times 10^3$  g/mol and 1.03, respectively.

### 2.2.1. Preparation of poly(2-(methacryloyloxy)ethyl phosphorylcholine)-*block*-poly((3-(methacryloylamino)propyl)trimethylammonium chloride) (PMPC<sub>20</sub>-*b*-PMAPTAC<sub>190</sub>)

PMPC macro-CTA (345 mg, 56.5  $\mu\text{mol}$ ,  $M_n$  (NMR) =  $6.21 \times 10^3$  g/mol,  $M_w/M_n=1.03$ ), 3-(methacryloylamino)propyl)trimethylammonium chloride (MAPTAC, 2.50 g, 11.3 mmol) and V-501 (7.90 mg, 28.2  $\mu\text{mol}$ ) were dissolved in 22.6 mL of water. The solution was deoxygenated by purging with Ar gas for 30 min. Block copolymerization was carried out at 70°C for 6 h. The diblock copolymer was purified by dialysis against pure water for 2 days. The zwitterionic-cationic diblock copolymer (PMPC<sub>20</sub>-*b*-PMAPTAC<sub>190</sub>; see structure in Fig. 1A) was recovered by a freeze-drying technique (2.46 g, 85.9%,  $M_n$ (NMR) =  $4.95 \times 10^4$  g/mol,  $M_w/M_n = 1.05$ ).

### 2.2.2. Preparation of poly(2-(methacryloyloxy)ethyl phosphorylcholine)-*block*-poly(sodium 2-(acrylamido)-2-methylpropanesulfonate) (PMPC<sub>20</sub>-*b*-PAMPS<sub>196</sub>)

A predetermined amount of 2-(acrylamido)-2-methylpropanesulfonic acid (AMPS, 2.00 g, 9.67 mmol) was neutralized with 1 M NaOH in 9.65 mL of water. To this solution was added PMPC macro-CTA (300 mg, 48.3  $\mu\text{mol}$ ,  $M_n$ (NMR) =  $6.21 \times 10^3$  g/mol,  $M_w/M_n = 1.03$ ) and V-501 (10.7 mg, 38.2  $\mu\text{mol}$ ). The solution was deoxygenated by purging with Ar gas for 30 min. Block copolymerization was carried out at 70°C for 3 h. The diblock copolymer was purified by dialysis against pure water for 2 days. The zwitterionic-anionic diblock copolymer (PMPC<sub>20</sub>-*b*-PAMPS<sub>196</sub>; see structure in Fig. 1A) was recovered by a freeze-drying technique (2.25 g, 97.0%,  $M_n$ (NMR) =  $4.85 \times 10^4$  g/mol,  $M_w/M_n = 1.07$ ).

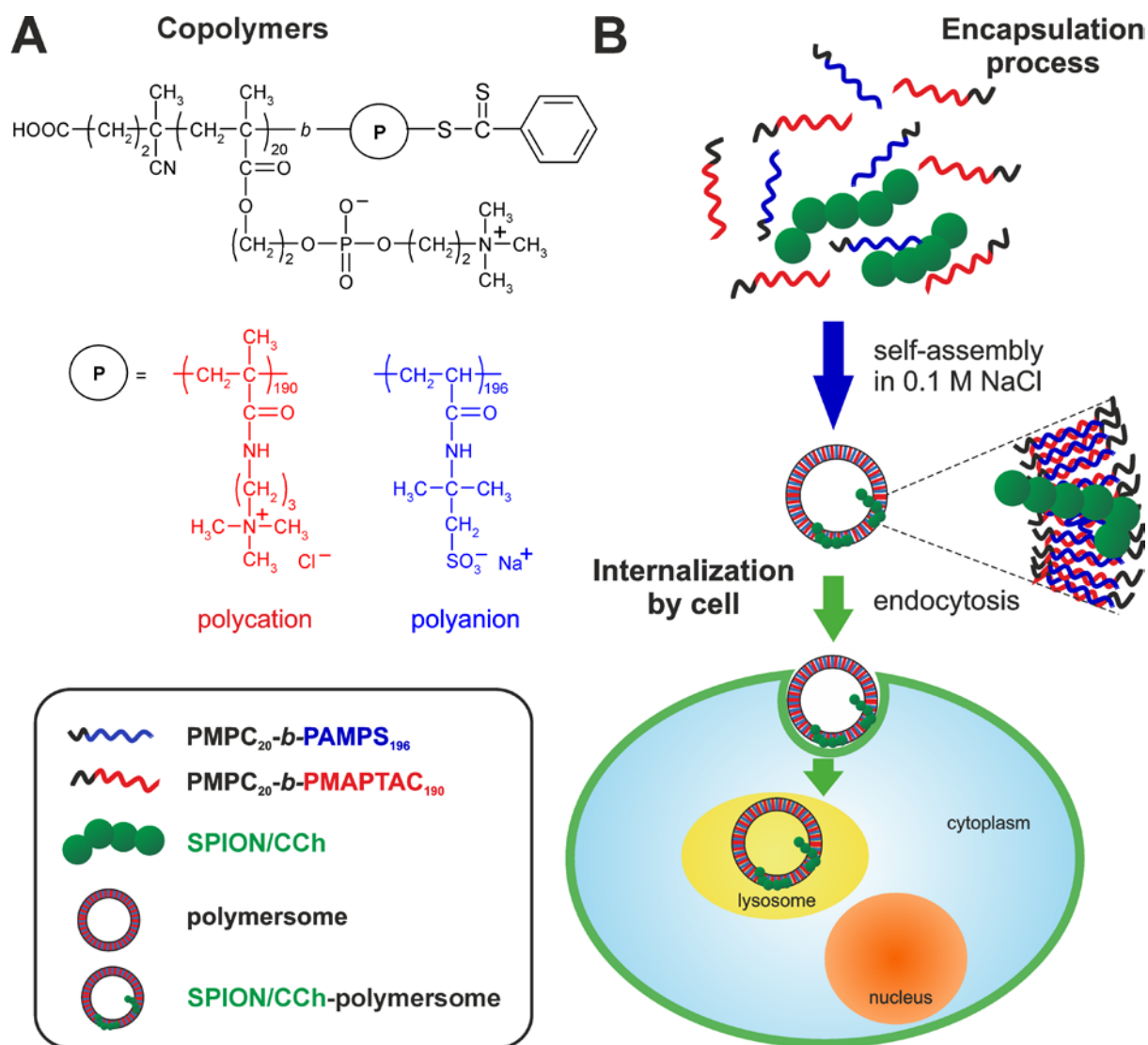


Fig. 1. (A) Molecular structures of the copolymers used for the preparation of polymersomes, PMPC<sub>20</sub>-b-PMAPTAC<sub>190</sub> and PMPC<sub>20</sub>-b-PAMPS<sub>196</sub>. (B) Schematic illustration of the encapsulation process of SPION/CCh in the polymersomes and the internalization of SPION/CCh-polymersomes by endothelial cells.

### 2.3. Synthesis of SPION/CCh

SPION coated with cationic chitosan derivative (SPION/CCh) were synthesized according to the method we have developed and described previously.<sup>33</sup> Briefly, iron salts at the molar ratio Fe(III):Fe(II) = 2:1 (0.1622 g FeCl<sub>3</sub>·6H<sub>2</sub>O and 0.0596 g FeCl<sub>2</sub>·4H<sub>2</sub>O) were

dissolved in 50 mL of 0.1 M sodium chloride solution of CCh ( $c = 3$  g/L). The solution was deoxygenated by purging with Ar and sonicated (Sonic-6, Polsonic, 480 W, 1 s pulse per 5 s break) for 10 min in a thermostated bath at 20 °C. Afterwards, 5 mL of 5 M  $\text{NH}_3(\text{aq})$  was added dropwise, and the solution was further deoxygenated and sonicated for 30 min at 20 °C. Finally, the SPION/CCh were purified by magnetic chromatography and the obtained suspension was filtered with PES syringe filters (0.2  $\mu\text{m}$ ).

#### 2.4. Modification of SPION/CCh with Alexa Fluor® 647 fluorescent probe

Immediately before modification, Alexa Fluor® 647 NHS Ester was dissolved in anhydrous *N,N*-dimethylformamide (DMF) to obtain a concentration of 10 mg/mL. 100  $\mu\text{L}$  of the dye solution was slowly added to 2 mL of the SPION/CCh suspension ( $c = 5$  mg  $\text{Fe}_3\text{O}_4/\text{mL}$ ) under stirring. The mixture was incubated for 1 h at room temperature with continuous stirring. After that time, the Alexa-labeled SPION/CCh particles were purified by dialysis against water at room temperature.

#### 2.5. Preparation of polymersomes

Polymersomes were prepared by mixing of two aqueous solutions of oppositely charged copolymers,  $\text{PMPC}_{20}\text{-}b\text{-PAMPS}_{196}$  and  $\text{PMPC}_{20}\text{-}b\text{-PMAPTAC}_{190}$ .  $\text{PMPC}_{20}\text{-}b\text{-PAMPS}_{196}$  and  $\text{PMPC}_{20}\text{-}b\text{-PMAPTAC}_{190}$  solutions in 0.1 M NaCl were prepared at a desired molar concentration, the same for both copolymers. Then, the solutions were mixed by adding dropwise the solution of  $\text{PMPC}_{20}\text{-}b\text{-PMAPTAC}_{190}$  to the solution of  $\text{PMPC}_{20}\text{-}b\text{-PAMPS}_{196}$  at room temperature. During this process, the system was vigorously stirred (800 rpm) and then it was equilibrated for at least 1 h prior to use in further studies. The ratio of block copolymers used to form the polymersomes was established to achieve complete charge neutralization.

That was reached when the mole fraction of the positively charged unit,

$$f^+ = \frac{[\text{MAPTAC}]}{[\text{MAPTAC}] + [\text{AMPS}]}, \text{ was equal to 0.5.}$$

## 2.6. Preparation of SPION/CCh-polyersomes

The CCh-coated SPION particles were incorporated into the polymeric bilayer at the initial stage of the vesicle preparation (Fig. 1B). Firstly, the SPION/CCh suspension ( $c_{\text{Fe}} = 542 \mu\text{g/mL}$ ) was sonicated for ca. 10 min at room temperature to disrupt any possible aggregates of nanoparticles. Then, the appropriate amount of the SPION/CCh suspension (calculated to achieve weight concentration of  $\text{Fe}_3\text{O}_4$  equal to 5% of the sum of  $\text{PMPC}_{20}\text{-}b\text{-PMAPTAC}_{190}$  and  $\text{PMPC}_{20}\text{-}b\text{-PAMPS}_{196}$  concentrations in the system) was added dropwise to the  $\text{PMPC}_{20}\text{-}b\text{-PAMPS}_{196}$  solution with simultaneous stirring of the system. Next, the solution of  $\text{PMPC}_{20}\text{-}b\text{-PMAPTAC}_{190}$  was added dropwise to the stirred mixture of  $\text{PMPC}_{20}\text{-}b\text{-PAMPS}_{196}$  and SPION/CCh. The molar ratio of block copolymers was the same as for the non-modified polyersomes ( $f^+ = 0.5$ ). The system ( $c_{\text{Fe}} = 103 \mu\text{g/mL}$ ) was equilibrated for at least 1 h and purified from nonencapsulated SPION/CCh by centrifugation (3 min, 6000 rpm). The supernatant containing SPION/CCh-polyersomes ( $c_{\text{Fe}} = 14 \mu\text{g/mL}$ ) was used for further studies. The fluorescently modified SPION/CCh were incorporated into the polymeric bilayer using the same procedure.

## 2.7. Characterization of SPION/CCh-polyersomes

The iron content in the resulting suspensions was determined using a spectrophotometric method based on the colored complex of Fe(II) with 1,10-phenanthroline. Briefly, iron oxide was decomposed by reaction with 3 M HCl. Then, an excess of ascorbic

acid (in relation to the expected iron content) was introduced in order to reduce Fe(III) to Fe(II). Finally, 3 mL of a 0.2% solution of 1,10-phenanthroline in 0.08 M HCl was added to the appropriately diluted solution of Fe(II) ions. The samples were left in the dark for 24 h, and their absorbance at 512 nm (characteristic of the formed complex) was measured. Based on the previously obtained calibration curve, the iron concentration in the samples were determined.

Cryo-transmission electron microscopy (cryo-TEM) was used to visualize the polymersomes (see Fig. 2). That technique allows for the least perturbing and direct imaging of the hydrated sample. The samples for cryo-TEM were prepared as described previously.<sup>34</sup> Briefly, 3  $\mu$ L of the studied colloidal dispersion was applied to an electron microscopy grid covered with perforated supporting film. Most of the sample was removed by blotting (Whattmann no. 1 filter paper) for approximately 1 s, and the grid was immediately plunged into liquid ethane held at  $-183^{\circ}\text{C}$ . The sample was then transferred without rewarming into a Tecnai Sphera G 20 electron microscope using a Gatan 626 cryo-specimen holder. The images were recorded at 120 kV accelerating voltage and microscope magnification ranging from 5000x to 9600x using a Gatan UltraScan 1000 slow scan CCD camera (giving a final pixel size from 2.0 to 0.7 nm) and low dose mode with the electron dose not exceeding 15 electrons per  $\text{\AA}^2$ . Typical value of applied underfocus ranged between 1.5 to 2.7  $\mu\text{m}$ . The applied blotting conditions resulted in specimen with thickness varying between 100 to ca. 300 nm.

A Zetasizer Nano ZS instrument (Malvern Instrument Ltd., Worcestershire, UK) was used for dynamic light scattering (DLS, Fig. 3) and zeta potential measurements. Samples were illuminated with a 633 nm laser, and the intensity of light scattered at an angle of  $173^{\circ}$  was measured. Measurements were performed at  $25^{\circ}\text{C}$ . The values of zeta potential, z-

average diameter (dz), polydispersity (PDI), and distribution profiles of the samples were calculated using software provided by the manufacturer.

Atomic force microscope (AFM) images (see Fig. 4 and 5) were obtained with Dimension Icon atomic force microscope (Bruker, Santa Barbara, CA) working in the air in a tapping mode. Magnetic force microscope (MFM) images were acquired using the same microscope working in a lift mode. In MFM measurements magnetic Co/Cr covered standard silicon cantilevers of normal spring constant of 2 N/m were used. Before scanning the cantilevers were magnetized with a small magnet. In QNM mode measurements standard silicon cantilevers of normal spring constant of 42 N/m were used (see Fig. S1 and S2 in ESI†). A sample for the measurements was prepared by placing a drop of the SPION/CCh-polymersome suspension on a silicon plate. After 1 h, the solvent was removed by purging with argon.

$^1\text{H}$   $T_1$  and  $T_2$  relaxation times (see Fig. S3 and S4 in ESI†) were measured on a Bruker BioSpec 9.4 T MRI system (Bruker, Germany) with a birdcage radio-frequency coil of the diameter equal to 36 mm. A probe was mounted on the animal bed and positioned in the centre of the magnet using standard positioning sequence (Tripilot). Before each experiment, the probe shimming and the pulse-lengths adjustments were made. Pulse adjustments and the consecutive relaxation time measurements were performed with the use of a TopSpin v. 2.1 software (Bruker, Germany) without gradient localization. The Inversion Recovery (IR) and standard Bruker Carr-Purcell-Meiboom-Gill (CPMG) sequences were used to measure  $T_1$  and  $T_2$ , respectively. Echo time in the CPMG experiments was equal to 10 ms for all measurements except the shortest  $T_2$  where it was set to 8 ms. Maximum number of  $\pi$  pulses changed from 20 for the shortest  $T_2$  to 708 for the pure water, with the number of consecutive experiments ranging from 8 to 24 respectively (one acquisition per experiment). 16 data points were measured in the IR experiment. They were uniformly distributed on the

logarithmic time scale, in the 0.4 – 18.9 s range. The repetition times were equal to 20 s for  $T_1$  measurements and 15 s for  $T_2$ . Two accumulations were used for both IR and CPMG acquisitions. Single-exponential curves were fitted in the time domain using specialized spectrometer procedures (TopSpin).

## 2.8. Cell viability assessment

*In vitro* cytotoxicity of SPION/CCh, polymersomes and SPION/CCh-polymersomes was measured using a 3-(4,5-dimethylthiazol-2-yl)-2,5-diphenyltetrazolium bromide (MTT) assay. Briefly, EA.hy926 cells were seeded in a 96-well plate at a density of 18000 cells per well. After 24 h incubation, a series of suspension dilutions (0.007 - 2.33  $\mu\text{g Fe/mL}$  for SPION/CCh and SPION/CCh-polymersomes; for the bare polymersomes, the total concentration of copolymers,  $c_p$ , was the same as for the SPION/CCh-polymersomes) was added into wells. After 72 h incubation, the cytotoxicity was measured using the MTT assay. The absorbance at 560 nm was measured using a microplate reader (Synergy 4, BioTek).

## 2.9. SPION/CCh-polymersomes intracellular uptake by endothelial cells

24 h before uptake study, EA.hy926 cells were seeded in 6-well plates with glass coverslips at the bottom. The cell monolayer was washed with Dulbecco's PBS and subsequently incubated with Alexa-labeled SPION/CCh-polymersomes (9  $\mu\text{g Fe/mL}$ ) in DMEM at 37 °C. After 24 h, the cells were washed twice with PBS and the nuclei were stained with Hoechst 33342 for 10 min. Then, the cells on the coverslips were fixed in 4% formaldehyde solution in PBS. The prepared specimens were observed using confocal laser scanning microscopy (CLSM). Images were acquired with an A1-Si Nikon (Japan) confocal

laser scanning system built onto a Nikon inverted microscope Ti-E using a Plan Apo 100×/1.4 Oil DIC objective. Two diode lasers (405 and 638 nm) were used for excitation. Images were acquired at a resolution of 1024 × 1024. Fluorescence and transmitted light images of the cells were collected.

### 3. Results and discussion

#### 3.1. Synthesis and characterization of SPION/CCh-polyersomes

Polymeric vesicles have been prepared using the procedure similar to the method developed previously for the formation of polymeric micelles from copolymers composed of PMPC and PAMPS or PMAPTAC blocks.<sup>35</sup> To obtain polyersomes rather than micelles the structure of the polymers, namely the ratio of the lengths of zwitterionic and charged blocks in the copolymers used, was adjusted accordingly. Very long negatively or positively charged blocks (PAMPS or PMAPTAC) and relatively short zwitterionic block (PMPC) promote vesicle formation. Oppositely charged blocks of copolymers attract each other and constitute the interior of the polyersome membrane, whereas zwitterionic blocks form its external and internal surfaces. SPION coated with the cationic derivative of chitosan can be easily incorporated into the polymeric membrane due to the electrostatic interactions with the negatively charged PAMPS blocks in the copolymer.

The cryo-TEM image of originally formed polyersomes (Fig. 2A) confirms the formation of the round vesicular structures. One can notice that diameters of polyersomes are in the range from 0.1 to 0.2 μm. The micrographs of SPION/CCh-polyersomes (Fig. 2B-D) demonstrate that SPION/CCh are present in the polymer membrane or inside the polyersome. As can be seen, the vesicles formed in the presence of SPION/CCh are larger and of more disperse size (ca. 0.1 – 0.4 μm) than non-modified polyersomes. The larger size

of vesicles containing SPION/CCh stems probably from the fact that SPION/CCh incorporated into the polymeric membrane are partially aggregated.

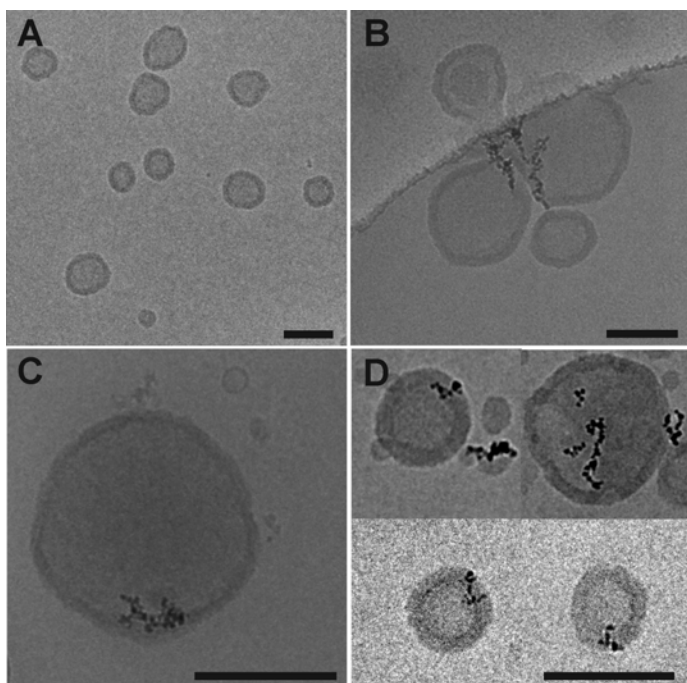


Fig. 2. The cryo-TEM micrographs for (A) polymersomes and (B-D) SPION/CCh-polymersomes. The scale bar represents 200 nm.

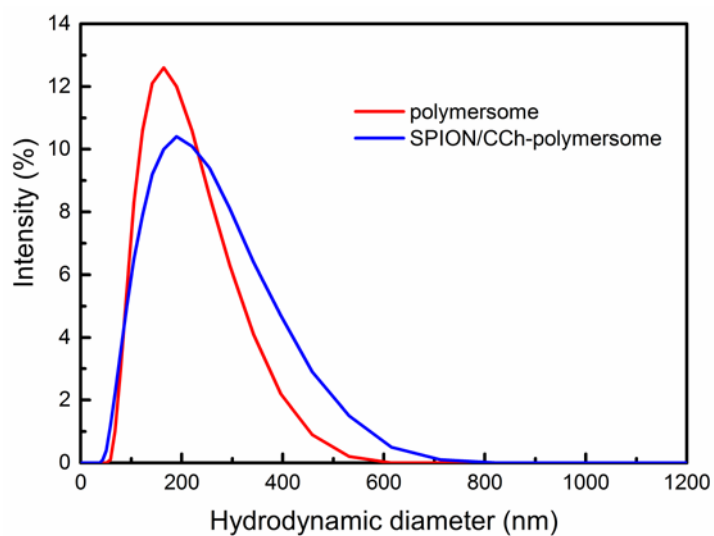


Fig. 3. Distribution profiles of the hydrodynamic diameters of polymersomes and SPION/CCh-polymersomes measured with DLS.

The scattering measurements were carried out to determine the hydrodynamic diameter of the polymersomes alone and of those incorporating SPION/CCh particles. The intensity weighted mean diameter ( $d_z$ ) of the vesicles determined with DLS was found to be in the range 160-170 nm, and the polydispersity was less than 0.2. Thus, the size distribution of the polymersomes was relatively narrow considering a simple method of their preparation. Fig. 3 shows hydrodynamic diameter distribution profiles of free polymersomes and SPION/CCh-polymersomes. The size profile for these vesicles was invariable for several days. As shown, the introduction of SPION/CCh (5% of copolymer mass) to the polymersomes caused changes in the size distribution of vesicles. The distributions became wider with a shoulder at the larger diameter region. The values of  $d_z$  increased to ca. 190 nm and PDI was higher than 0.2.

Zeta potential values measured for both SPION/CCh-polymersomes and non-modified polymersomes are very similar and equal approximately to 0 mV (Table 1). Zeta potential observed for SPION/CCh is strongly positive (ca. +40 mV). The fact that the surface of the polymersomes is uncharged indicates that it is indeed composed of zwitterionic blocks. Very similar charge measured for polymersomes containing SPION/CCh proves that SPION/CCh are located within polymeric membrane and/or inside the vesicle. That confirms that SPION/CCh are incorporated into the polymersome and that the purification procedure applied to the system was effective. Moreover, the lack of high charge on the vesicle surface significantly reduces the probability that the SPION/CCh-polymersomes are rapidly cleared due to enhanced hepatic uptake.<sup>36</sup>

Table 1. Zeta potential values for SPION/CCh, polymersome and SPION/CCh-polymersome dispersions.

Sample	Zeta potential (mV)
SPION/CCh	$+39.4 \pm 8.4$
Polymersome	$-4.0 \pm 5.8$
SPION/CCh-polymersome	$+3.1 \pm 6.6$

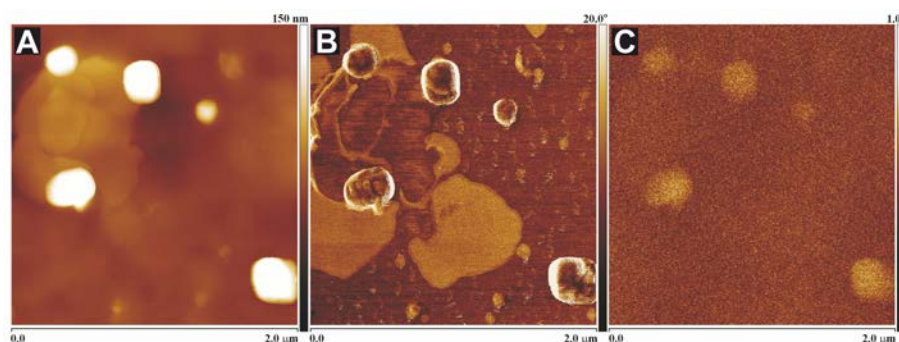


Fig. 4. AFM images of SPION/CCh-polymersomes. (A) Topography, (B) AFM phase, (C) MFM phase.

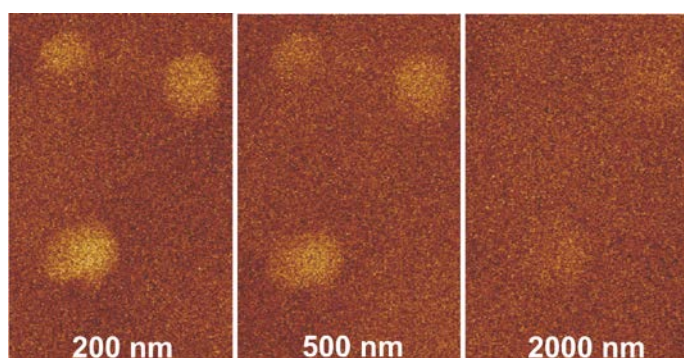


Fig. 5. MFM phase images of SPION/CCh-polymersomes in three different lift distances (surface – microscope tip distance).

MFM was used to confirm the magnetic properties of the SPION/CCh-polymerosomes. The microscope worked in the interleaved mode, resulting in an AFM topography, phase image and MFM magnetic phase image for exactly the same area of the sample. All SPION/CCh-polymerosomes, which were shown in the AFM image, produced a signal in the MFM phase image as well (Fig. 4). That can occur only when a sample possesses magnetic domains, which are able to interact with the magnetized tip and clearly suggested that the investigated sample was magnetic. Moreover, the MFM magnetic phase images were obtained at three different lift distances (*i.e.*, surface – microscope tip distance): 200, 500 and 2000 nm (Fig. 5). It was observed that an increase in the distance caused weakening of the magnetic signal in the MFM phase image. This behavior indicates that the values of magnetic forces are strongly dependent on the distance between two magnetic domains. It is yet another confirmation that the SPION/CCh-polymerosomes exhibit magnetic properties.

SPION can be used as a  $T_2$  contrast agent in MRI, if the contrast enhancement occurs as a result of the interaction between contrast agents and neighboring water protons.<sup>37</sup> Therefore, it was important to prepare polymerosomes with semipermeable membrane allowing water molecules to diffuse in. To evaluate the possibility of application of SPION/CCh-polymerosomes in MRI we determined their relaxivities and compared these values to a commercially available MRI contrast agent, SHP-20.  $^1\text{H}$   $T_1$  and  $T_2$  relaxation times were measured for samples containing various concentrations of iron (0 – 4  $\mu\text{g Fe/mL}$ ) and the relaxivities  $r_1$  and  $r_2$  were calculated using the following relations:

$$R_1 = \frac{1}{T_1} \quad R_2 = \frac{1}{T_2} \quad (1)$$

$$R_1 = R_1^0 + r_1 c_{\text{m,Fe}} \quad R_2 = R_2^0 + r_2 c_{\text{m,Fe}} \quad (2)$$

where  $R_1(R_2)$  is the longitudinal (transverse) relaxation rate;  $T_1(T_2)$  is the longitudinal (transverse) relaxation time;  $R_1^0(R_2^0)$  is the longitudinal (transverse) relaxation rate in the absence of the contrast media;  $r_1(r_2)$  is the longitudinal (transverse) relaxivity; and  $c_{m,Fe}$  is the molar iron concentration in the samples (see Fig. S3 and S4 in ESI†). As shown in Table 2, high  $r_2$  relaxivity values and low  $r_1$  values obtained for SPION/CCh and SPION/CCh-polymersomes confirm the ability of these structures to extend shorten  $T_2$  relaxation time in MRI. In comparison with SHP-20, the  $r_2$  values for SPION/CCh and SPION/CCh-polymersomes are much higher, even twice in the case of SPION/CCh-polymersomes. This is the desired effect, because the injected dose of the contrast agent may be reduced without adversely affecting the contrast enhancement in MRI. In the case of SPION/CCh, the increase in the  $r_2$  values may be explained by the presence of the hydrophilic polymer (CCh) surrounding iron oxide nanocrystals as the coating, because the more hydrated coating, the more decreased the water diffusion coefficient.<sup>38</sup> So, water diffusion may be hampered by the hydrophilic polymer layer causing enhancement effect.<sup>39</sup> The incorporation of SPION/CCh into the mixed polyelectrolyte membrane of the vesicles resulted in further significant increase of  $r_2$  value (see Fig. 1B). The transverse relaxivity of SPION/CCh-polymersomes is comparable to that reported by Hickey et al.<sup>14</sup> for SPION incorporated into polymersomes made of a block copolymer of poly(acrylic acid) and polystyrene (PAA-b-PS). The  $r_2$  value of the 241 nm magneto-polymersomes was determined to be  $555 \pm 24 \text{ mM}^{-1} \text{ s}^{-1}$  and the authors concluded that this is the highest value reported so far for the superparamagnetic iron oxide particles.

Table 2. Relaxivity values for SPION/CCh, SPION/CCh-polymersome and the commercial MRI contrast agent (SHP-20, Ocean NanoTech) at 9.4 T.

Sample	$r_1$ (mM <sup>-1</sup> s <sup>-1</sup> )	$r_2$ (mM <sup>-1</sup> s <sup>-1</sup> )
SPION/CCh	1.31 ± 0.17	372 ± 12
SPION/CCh-polymersome	1.09 ± 0.18	573 ± 10
SHP-20	-	259 ± 16

### 3.2. Cell viability assessment

The MTT assay was performed to examine cytotoxicity of the obtained SPION/CCh, polymersomes and SPION/CCh-polymersomes. As shown in Fig. 6, the bare polymersomes did not significantly affect the endothelium viability in the studied range of concentrations as evidenced by the MTT assay. The PMPC units present in the polymers used for the preparation of the polymersomes are biocompatible.<sup>40,41</sup> Phosphorylcholine (PC) is a zwitterionic group present at the end of certain phospholipids and thus on the external surface of cell membranes. In the case of the polymersomes the same groups are exposed to the aqueous phase, therefore they can mimic biomembranes. On the other hand, SPION/CCh tended to decrease the viability to ca. 90% of control even at the lowest concentrations. This slight decrease in the cell viability is likely caused by the presence of CCh on the SPION/CCh surface. It is known that chitosan derivatives modified with GTMAC (containing quaternary ammonium groups) can be cytotoxic to various cells;<sup>42,43</sup> the cytotoxicity of these polymers increases with growing degree of quaternization. In turn, the incorporation of SPION/CCh within the polymersome membrane increased the viability of endothelial cells. Our data indicate that SPION/CCh-polymersomes are not cytotoxic to endothelium up to the concentration of 0.7 µg Fe/mL.

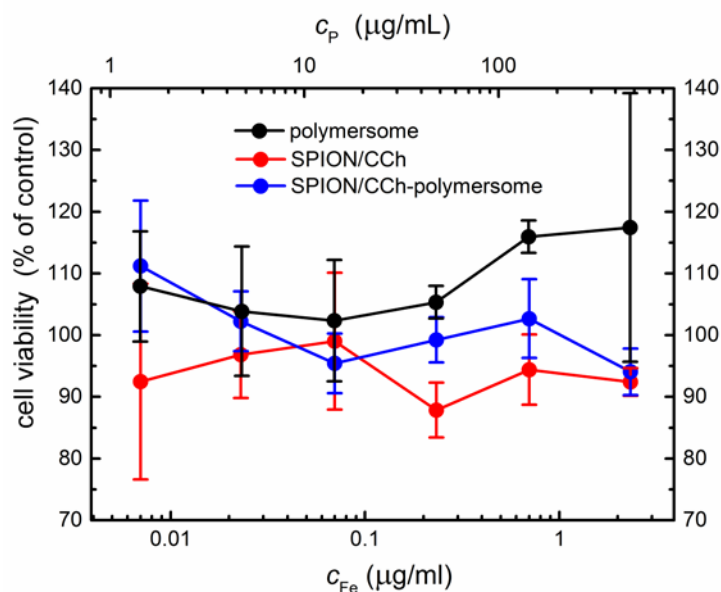


Fig. 6. Effect of polymersomes, SPION/CCh, and SPION/CCh-polymersomes on cell viability. The EA.hy926 cells were treated with the agents for 72 h before the MTT assay. Data are presented as the mean  $\pm$  SD ( $n = 4$ ).

### 3.3. SPION/CCh-polymersomes intracellular uptake by endothelial cells

The intracellular uptake of fluorescently modified SPION/CCh-polymersomes was studied using the CLSM imaging. As shown in Fig. 7, red fluorescence characteristic of the fluorescently modified SPION/CCh-polymersomes material is emitted from the inside of EA.hy926 cells, whose shapes were determined by the transmitted light microscopy observation of the same sample. Hoechst dye was used to stain the nuclei of the observed cells (blue fluorescence). Based on these observations it can be concluded that the SPION/CCh-polymersomes were effectively internalized by EA.hy926 cells. Although we have neither studied the mechanism of polymersomes endothelial uptake, nor analyzed whether this process is mediated by endocytosis, we suggest that polymersomes-based nanoparticles offer a unique system to be exploited as a delivery system to endothelium.

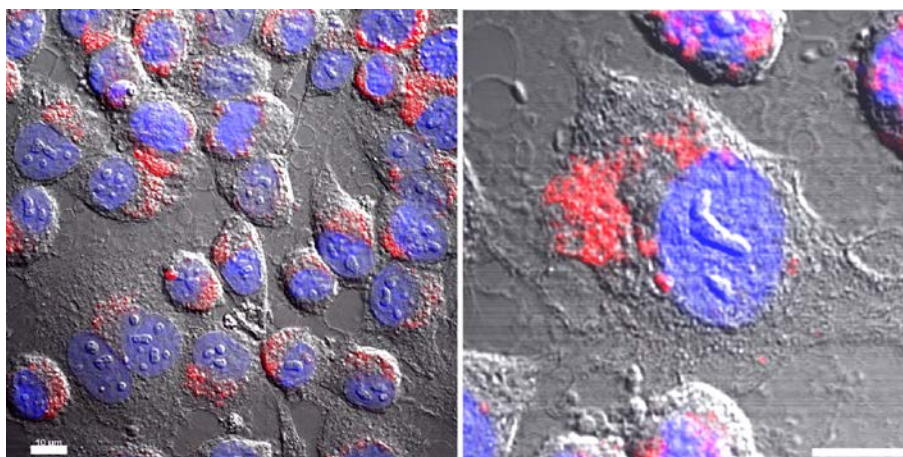


Fig. 7. Internalization of fluorescently modified SPION/CCh-polymerosomes (red ones) by EA.hy926 cells observed using CLSM. The nuclei were stained with Hoechst 33342 (blue). The scale bar corresponds to 10  $\mu\text{m}$ .

#### 4. Conclusions

In the present study, we demonstrated for the first time that stable polymerosomes with the semipermeable membrane can be prepared based on the pair of oppositely charged copolymers containing ionic and zwitterionic blocks. Such polymerosomes with the ionic membrane core are able to accumulate highly charged nanoparticles like SPION coated with a cationic chitosan derivative. The SPION/CCh-polymerosomes possess excellent magnetic properties and shorter  $T_2$  relaxation time in MRI compared to the commercial contrast agent. This suggests their potential application as the  $T_2$  contrast agent. Moreover, they are not toxic and small enough to be internalized by endothelial cells. Based on these results one can expect that the PMPC-based polymerosomes with SPION/CCh could prove useful as the MRI

contrast agent, while the polymersome nanostructures may be well suited for drug delivery to endothelium.

### Acknowledgments

This work was supported by the European Union from the resources of the European Regional Development Fund under the Innovative Economy Program (grant coordinated by JCET-UJ, No POIG.01.01.02-00-069/09). This work was also financially supported by a Grant-in-Aid for Scientific Research (25288101) from the Japan Society for the Promotion of Science (JSPS) and the Cooperative Research Program Network Joint Research Center for Materials and Devices (2013B25). The research was carried out with the equipment purchased thanks to the financial support of the European Regional Development Fund in the framework of the Polish Innovation Economy Operational Program (contract No POIG.02.01.00-12-023/08). J.B. acknowledges the support of the grants P302/12/G157, PRVOUK P27/LF1/1 and UNCE 204022, OPVK-CZ.1.07/2.3.00/30.0030), and OPPK-CZ.2.16/3.1.00/24010.

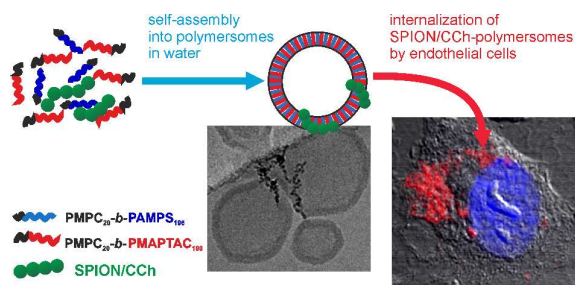
### References

- 1 B. M. Discher, Y-Y. Won, D. S. Ege, J. C-M. Lee, F. S. Bates, D. E. Discher, D. A. Hammer, *Science*, 1999, 284, 1143–1146.
- 2 K. Balakumar, K. Vamshikrishna, C. Vijaya Raghavan, S. Karthik, N. Tamilselvan, G. Marslin, *J. Drug Target.*, 2014, 22, 469–477.
- 3 G-Y. Liu, C-J. Chen, J. Ji, *Soft Matter*, 2012, 8, 8811–8821.
- 4 R. J. Hickey, A. S. Haynes, J. M. Kikkawa, S-J. Park, *J. Am. Chem. Soc.*, 2011, 133, 1517–1525.

- 5 M. Joglekar, B. G. Trewyn, *Biotechnol. J.*, 2013, 8, 931–945.
- 6 F. Meng, Z. Zhong, J. Feijen, *Biomacromolecules*, 2009, 10, 197–209.
- 7 A. Feng, J. Yuan, *Macromol. Rapid Commun.*, 2014, 35, 767–779.
- 8 H. De Oliveira, J. Thevenot, S. Lecommandoux, *WIREs Nanomed. Nanobiotechnol.*, 2012, 4, 525–546.
- 9 J. Du, Y. Tang, A. L. Lewis, S. P. Armes, *J. Am. Chem. Soc.*, 2005, 127, 17982–17983.
- 10 R. R. Maddikeri, S. Colak, S. P. Gido, G. N. Tew, *Biomacromolecules*, 2011, 12, 3412–3417.
- 11 A. Koide, A. Kishimura, K. Osada, W-D. Jang, Y. Yamasaki, K. Kataoka, *J. Am. Chem. Soc.*, 2006, 128, 5988–5989.
- 12 M. W. Freeman, A. Arrott, J. H. L. Watson, *J. Appl. Phys.*, 1960, 31, S404–405.
- 13 Z. Cheng, D. L. J. Thorek, A. Tsourkas, *Adv. Funct. Mater.*, 2009, 19, 3753–3759.
- 14 R. J. Hickey, J. Koski, X. Meng, R. A. Riggleman, P. Zhang, S-J. Park, *ACS Nano*, 2014, 8, 495–502.
- 15 M. Krack, H. Hohenberg, A. Kornowski, P. Lindner, H. Weller, S. Förster, *J. Am. Chem. Soc.*, 2008, 130, 7315–7320.
- 16 H. Oliveira, E. Pérez-Andrés, J. Thevenot, O. Sandre, E. Berra, S. Lecommandoux, *J. Controlled Release*, 2013, 169, 165-170.
- 17 W-H. Chiang, W-C. Huang, C-W. Chang, M-Y. Shen, Z-F. Shih, Y-F. Huang, S-C. Lin, H-C. Chiu, *J. Controlled Release*, 2013, 168, 280-288.
- 18 M. Muthiah, S. J. Lee, M. Moon, H. J. Lee, W. K. Bae, I. J. Chung, Y. Y. Jeong, I-K. Park, *J. Nanosci. Nanotechnol.*, 2013, 13, 1626–1630.
- 19 A. A. Kuznetsov, V. I. Filippov, T. A. Nikolskaya, A. P. Budko, A. L. Kovarskii, S. V. Zontov, B. Y. Kogan, O. A. Kuznetsov, *J. Magn. Magn. Mater.*, 2009, 321, 1575–1579.

- 20 C. Sanson, O. Diou, J. Thévenot, E. Ibarboure, A. Soum, A. Brûlet, S. Miraux, E. Thiaudière, S. Tan, A. Brisson, V. Dupuis, O. Sandre, S. Lecommandoux, *ACS Nano*, 2011, 5, 1122–1140.
- 21 R. Bleul, R. Thiermann, G. U. Marten, M. J. House, T. G. S. Pierre, U. O. Häfeli, M. Maskos, *Nanoscale*, 2013, 5, 11385–11393.
- 22 L. Pourtau, H. Oliveira, J. Thevenot, Y. Wan, A. R. Brisson, O. Sandre, S. Miraux, E. Thiaudiere, S. Lecommandoux, *Adv. Healthcare Mater.*, 2013, 2, 1420–1424.
- 23 X. Su, S. K. M. Moinuddeen, L. Mori, M. Nallani, *J. Mater. Chem. B*, 2013, 1, 5751–5755.
- 24 M. A. Gimbrone Jr., G. García-Cardeña, *Cardiovasc. Pathol.*, 2013, 22, 9–15.
- 25 J. A. Vita, J. F. Keaney Jr., *Circulation*, 2002, 106, 640–642.
- 26 S. Chłopicki, R. J. Gryglewski, *Pharmacol. Rep.*, 2005, 57, Suppl:86–96.
- 27 A. Scherpereel, R. Wiewrodt, M. Christofidou-Solomidou, R. Gervais, J. C. Murciano, S. M. Albelda, V. R. Muzykantov, *Fed. Am. Soc. Exp. Biol. J.*, 2001, 15, 416–426.
- 28 R. Stahn, C. Grittner, R. Zeisig, U. Karsten, S. B. Felix, K. Wenzel, *Cell. Mol. Life Sci.*, 2001, 58, 141–147.
- 29 J. Cho, J. Grant, M. Piquette-Miller, C. Allen, *Biomacromolecules*, 2006, 7, 2845–2855.
- 30 Y. Mitsukami, M. S. Donovan, A. B. Lowe, C. L. McCormick, *Macromolecules*, 2001, 34, 2248–2256.
- 31 C. J. Edgell, C. C. Mcdonald, J. B. Graham, *Cell Biol.*, 1983, 80, 3734–3737.
- 32 S. Yusa, K. Fukuda, K. Yamamoto, K. Ishihara, Y. Morishima, *Biomacromolecules*, 2005, 6, 663–670.
- 33 A. Szpak, G. Kania, T. Skórka, W. Tokarz, S. Zapotoczny, M. Nowakowska, *J. Nanopart. Res.*, 2013, 15, 1372.

- 34 J. Dubochet, M. Adrian, J. J. Chang, J. C. Homo, J. Lepault, A. W. McDowell, P. Schultz, *Rev. Biophys.*, 1988, 21, 129–228.
- 35 K. Nakai, M. Nishiuchi, M. Inoue, K. Ishihara, Y. Sanada, K. Sakurai, S-I. Yusa, *Langmuir*, 2013, 29, 9651–9661.
- 36 J. S. Lee, J. Feijen, *J. Controlled Release*, 2012, 161, 473–483.
- 37 H. B. Na, I. C. Song, T. Hyeon, *Adv. Mater.*, 2009, 21, 2133–2148.
- 38 S. Kwak, M. Lafleur, *Macromolecules*, 2003, 36, 3189–3195.
- 39 H. W. de Haan, C. Paquet, *Magn. Reson. Med.*, 2011, 66, 1759–1766.
- 40 D. Chapman, *Langmuir*, 1993, 9, 39–45.
- 41 G-Y. Liu, L-P. Lv, C-J. Chen, X-F. Hu, J. Ji, *Macromol. Chem. Phys.*, 2011, 212, 643–651.
- 42 J. Kowapradit, P. Opanasopit, T. Ngawhirunpat, A. Apirakaramwong, T. Rojanarata, U. Ruktanonchai, W. Sajomsang, *AAPS PharmSciTech*, 2010, 11, 497–508.
- 43 B. Xiao, Y. Wan, X. Wang, Q. Zha, H. Liu, Z. Qiu, S. Zhang, *Coll. Surf. B*, 2012, 91, 168–174.



Novel biocompatible polymersomes with semipermeable ionic membrane were used as the promising delivery system of superparamagnetic iron oxide nanoparticles (SPION), contrast agents for MRI.